UNIVERSITAT POLITÈCNICA
DE CATALUNYA

Experiments on generation and conversion

Carles Batlle, Arnau Dòria Cerezo,
Enric Fossas, Romeo Ortega

ACES: Control Avançat de Sistemes d'Energia

IOC-DT-P-2006-15
Abril 2006

Institut d'Organització i Control
de Sistemes Industrials

Experiments on Generation and Conversion.

Carles Batlle, Arnau Dòria-Cerezo and Enric Fossas
Institut d'Organització i Control de Sistemes Industrials
Universitat Politècnica de Catalunya
Romeo Ortega
Laboratoire des Signau et Systémes
Supélec

April, 2006

Abstract

Experimental results of the Flywheel Energy Storage System are presented. This report finalizes the work of the UPC in the context of the GeoPlex European project. This document contains only the experimental results of the system, while the associated theoretical results and simulations are presented in previous works.

The experimental results validates the policy management, the Port-Hamiltonian models and the developed controllers using the IDA-PBC approach along the project.

Keyboards: Flywheel Energy Storage System, power flow management.

Paraules clau: Sistema d'emmagatzement d'energia cinètica, gestió de flux de potència.

Palabras clave: Sistema de almacenamiento de energía cinética, gestión del flujo de potencia.

Contents

1 Introduction

The system studied in this workpackage is an autonomous energy–switching system that regulates the energy flow between a local prime mover (a flywheel) and the electrical power network, in order to satisfy the demand of a time–varying electrical load. This system, used in the CERN (Centre Européen pour la Recherche Nucléaire) to store electrical energy for the particle accelerator or at the Okinawa Electric Power Company [1], has been also studied in [1]. The main goal of the system is, basically, to store kinetic energy into a flywheel and deliver it when an external load requires a high energy flow.

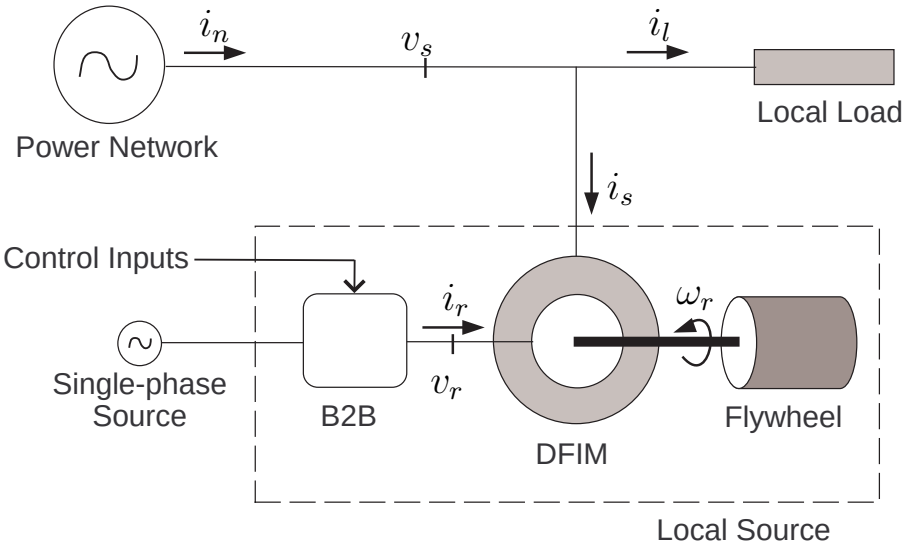

Figure 1: Doubly fed induction machine coupled to a flywheel, controlled by a back-to-back converter and connected to a power network and a load.

The system (see Figure 1) is composed by a doubly–fed induction machine (DFIM) coupled to a flywheel and controlled through the rotor windings by a back-to-back converter (B2B). This is the most common control architecture of the DFIM [1][6][7][8][9][10][11][12] , typically achieved by means of a B2B. In a case that the AC source of the B2B is connected to the 3-phase power grid, this architecture is also known as Scherbius Drive [7], *i.e.* the power converter is in a closed–loop with the DFIM. In practice, due to the fact that the power flowing through the power converter is smaller than the power flowing to the DFIM stator side, it is common to neglect this *feedback* connection.

The DFIM is controlled through the rotor windings port ($v_r, i_r \in \mathbb{R}^3$, where v and i are a three-phase voltage and current variables, and subindex r refers to the rotor). It is coupled to an energy–storing flywheel with port variables (τ_e electrical torque, ω mechanical speed). An electrical network modelled by an ideal AC voltage source with port variables ($v_n, i_n \in \mathbb{R}^3$ subindex n refers to the network variables), and a generic electrical three-phase load, represented by its impedance Z_l, is connected to the stator port variables ($v_s, i_s \in \mathbb{R}^3$).

As mentioned above, the main objective of the system is to supply the required power to the load with a high network power factor. Depending on the load demands, the DFIM acts as an energy–switching device between the flywheel and the electrical power network. The control problem is to optimally regulate the power flow.

These goals, assuming a maximal active power of the network P_n^{MAX}, can be summarized as follows:

- **To supply** the extra energy required by the load. Notice that this objective concerns the active power, and considering a constant grid voltage, $V_n = ct$, this requirement is achieved by the stator currents.
- **To store** kinetic energy in the flywheel when the load does not require all the grid power.
- **To compensate** the power factor ($\cos\phi$), i.e., the whole system (load and local source acts as a pure resistor). That is $\cos\phi \sim 0$, or, in other words assuming, sinusoidal waveform and an equilibrated system, this objective can be written as $Q_n \sim 0$.

This control problem can be achieved by commuting between different steady–state regimes. The switching strategy was studied in [2].

2 Switching strategy

The switching policy of the Flywheel Energy Storage System is studied and validated by simulations in [2]. The power management schedule is determined according to the considerations presented in Section 1. The general goal is to supply the required power to the load with a high network power factor, *i.e.*, $Q_n \sim 0$. On the other hand, we show in [2] that the DFIM has an optimal mechanical speed ω^* for which there is minimal power injection through the rotor ($\omega^* = \omega_s$). Combining these two factors suggests to consider the following three modes of operation:

- **Generator mode.** When the real power required by the local load is bigger than the maximum network power (say, P_n^M) we use the DFIM as a generator. In this case we fix the references for the network real and reactive powers as $P_n^* = P_n^M$ and $Q_n^* = 0$.
- **Storage (or motor) mode.** When the local load does not need all the network power and the mechanical speed is far from the optimal value the "unused" power network is employed to accelerate the flywheel. From the control point of view, this operation mode coincides with the *generator mode*, and thus we fix the same references—but now we want to extract the maximum power from the network to transfer it to the flywheel.
- **Stand-by mode.** Finally, when the local load does not need all the power network and the mechanical speed is near to the optimal one we just compensate for the flywheel friction losses by regulating the speed and the reactive power. Hence, we fix the reference for the mechanical speed at its minimum rotor losses value (to be defined below) and set $Q_n^* = 0$.

The operation modes boil down to two kinds of control actions as expressed in Table 1, where P_l is the load power and $\epsilon > 0$ is some small parameter.

$P_n^* < P_l$	$\lvert\omega - \omega^*\rvert \leq \epsilon$	Mode	References
True	True	Generator	$P_n^* = P_n^M$ and $Q_n^* = 0$
True	False	Generator	$P_n^* = P_n^M$ and $Q_n^* = 0$
False	True	Stand-by	$Q_n^* = 0$ and $\omega^* = \omega_s$
False	False	Storage	$P_n^* = P_n^M$ and $Q_n^* = 0$

Table 1: Control action table.

3 Experimental Results

In this section we present the experimental setup and the experimental results of the Flywheel Energy Storage System.

3.1 Experimental setup

The experimental setup is described extensively in [3]. Figure 2 shows the DFIM coupled to a flywheel and the local load. In order to increase the range of available parameters in the experimental setup the flywheel is split into two separate inertias.

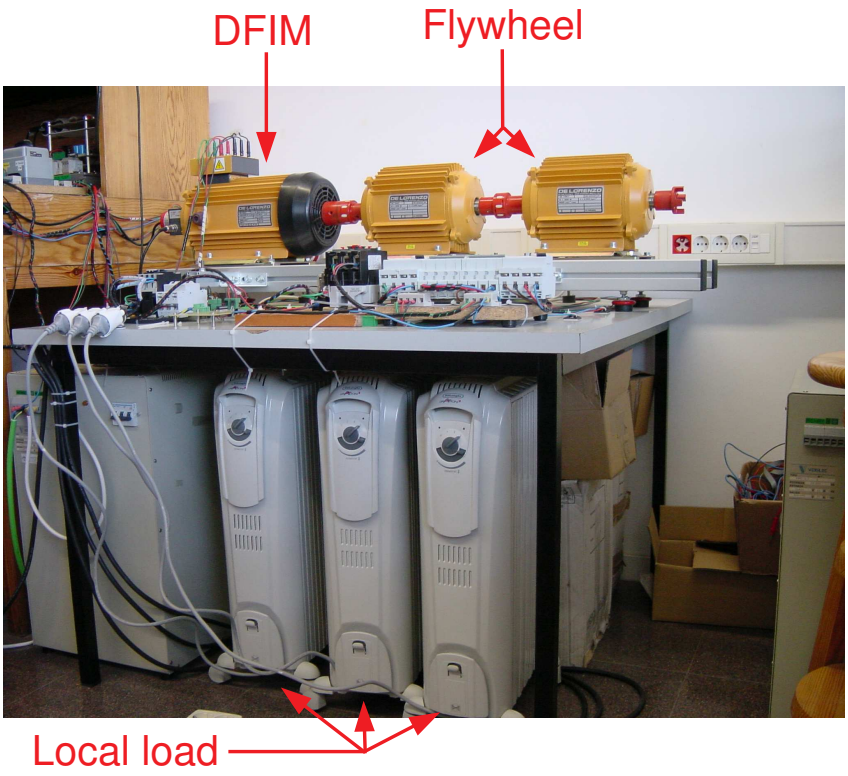

Figure 2: The DFIM coupled to a flywheel.

- The DFIM is a 1.1kW machine De Lorenzo DL 1022K, with the following parameters: number of poles $n = 2$, voltage fed 220/380V (Δ/Y), nominal current 4.8/2.8A

(Δ/Y), stator resistance $R_s = 4.92\Omega$, rotor resistance $R_r = 4.42\Omega$, mutual inductance $L_{sr} = 710$mH, stator inductance $L_s = 725$mH, rotor inductance $L_r = 715$mH, mechanical damping $B_r = 0.005$Kg m^{2}s^{-1} and inertia $J_d = 0.00512$Kg m^2.

- The flywheels have a moment of inertia $J_f = 0.055$Kg m^2 each one, which gives a total inertia $J_m = 0.11512$Kg m^2.
- The local load is made up of three variable resistors $R = 37/68/89\Omega$.

The back-to-back converter is depicted in Figure 3 and has the following parts:

- A full-bridge boost converter (depicted in Figure 3) with IGBT switches (Siemens BSM 25GD 100D) and parameters: $r = 0.1\Omega$, $L = 1$mH, $C = 4500\mu$F. The switching frequency of the converter is 20 KHz and a synchronous centered-pulse single-update pulse-width modulation strategy is used to map the controller's output to the IGBT gate signals.
- A 3-phase DC/AC inverter with a set of IGBT switches (1200 V, 100 A). The switching frequency of the inverter is 20 KHz and a synchronous centered-pulse single-update pulse-width modulation strategy is used to map the controller's output to the IGBT gate signals.
- The analog circuitry for the sensors: the AC main source, PMW and DC bus voltages and currents are sensed with isolation amplifiers. All the signals from the sensors pass through the corresponding gain conditioning stages to adapt their values to A/D converters.
- Control hardware and DSP implementation: the control algorithm can be implemented using the Analog Devices DSP-21116 and DSP-21992 processors. The processing core of this device runs at 100MHz and has a 32bit floating-point unit. The sampling rate of the A/D channels has been selected at 20kHz, the same as the switching frequency of the full-bridge system.
- The nominal RMS AC mains voltage is $V_s = 48.9$V RMS and its nominal frequency is 50 Hz.

The control algorithm is coded into a computer running with RTLinux (Real Time Linux), using RTiC-Lab (Real Time Controls Laboratory) [5].

The control hardware setup consists of:

- PC computer: Pentium IV, 1.8 GHz, 512MB RAM.
- A/D card: 3 PCI-DAS 4020/12 modules. Ultra High-Speed PCI-bus Compatible, 4-Channel, 12-Bit Analog Input Board with two Analog Output Channels and 24 Digital I/O Channels.
- PWM card: NuDAQ PCI-8133. 3-Channel quadrature encoder counters for a PCI PnP-bus and a 12-Bit PWM waveform generators.

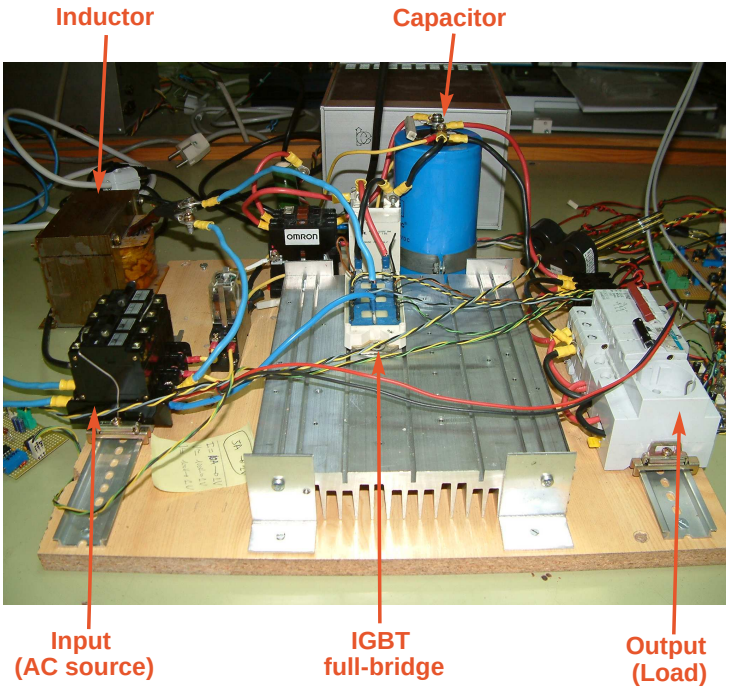

Figure 3: Experimental setup: full-bridge rectifier, DSP card, sensors, data acquisition.

3.2 Experimental results

Experimental results are shown in Figures 4-8. The maximal power network delivered by the load is fixed at $P_n = 3300$W. The DFIM starts at the optimal speed ($\omega = 314$rad s^{-1}). A resistive load, which requires $P_l = 4180$W is connected for 1 second.

Figure 4 shows that the power delivered by the load remains close to the desired value even if the connected load requires more power. This is due to the fact that the mechanical speed of the DFIM (and the flywheel) decreases, Figure 5, providing thus the required extra energy, and when the load is disconnected the mechanical speed returns to the optimal value.

The dq stator currents are depicted in Figure 6. Since the stator voltage reference is used to transform the original variables, i_{sd} represents the active power flowing through the stator side of the DFIM and i_{sq} the reactive power. It can be seen that the reactive power supplied by the grid is close to zero (the local load is purely resistive and the DFIM only consumes active power).

Finally Figures 7 and 8 show the control action u_r and the corresponding a-phase of the rotor voltages, V_{ra}.

Further experiments can be found in the Arnau Dòria-Cerezo Ph.D dissertation [4], scheduled for presentation in September 2006.

4 Conclusions

We presented the experimental results of the Flywheel Energy Storage System. The results validate the power flow management and the switching policy in order to achieve the main

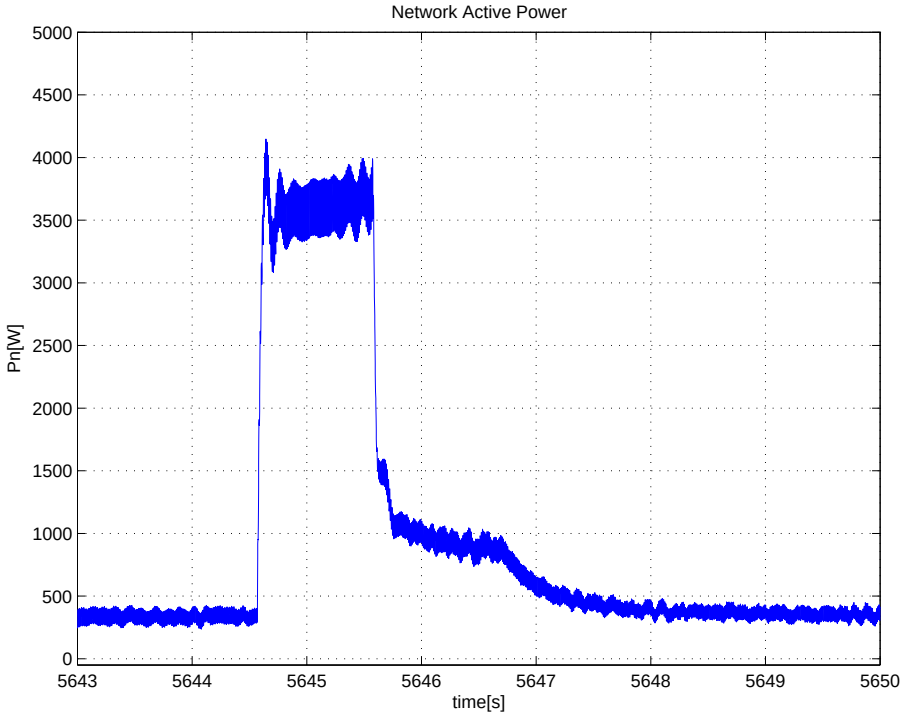

Figure 4: Experimental results: network active power, P_n.

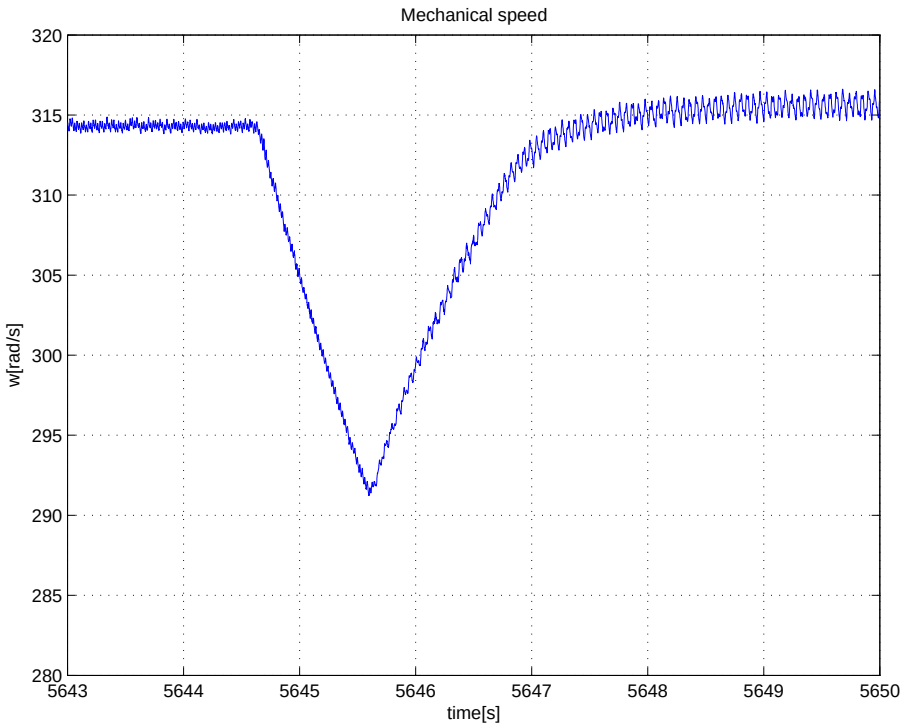

Figure 5: Experimental results: mechanical speed, ω.

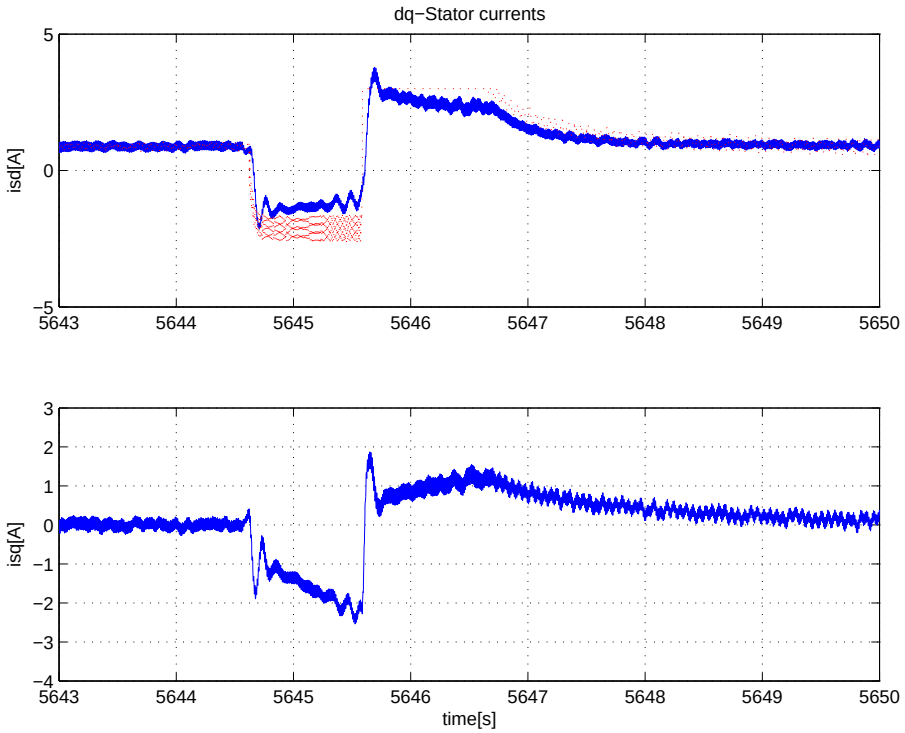

Figure 6: Experimental results: stator dq-currents, i_{sd} and i_{sq}.

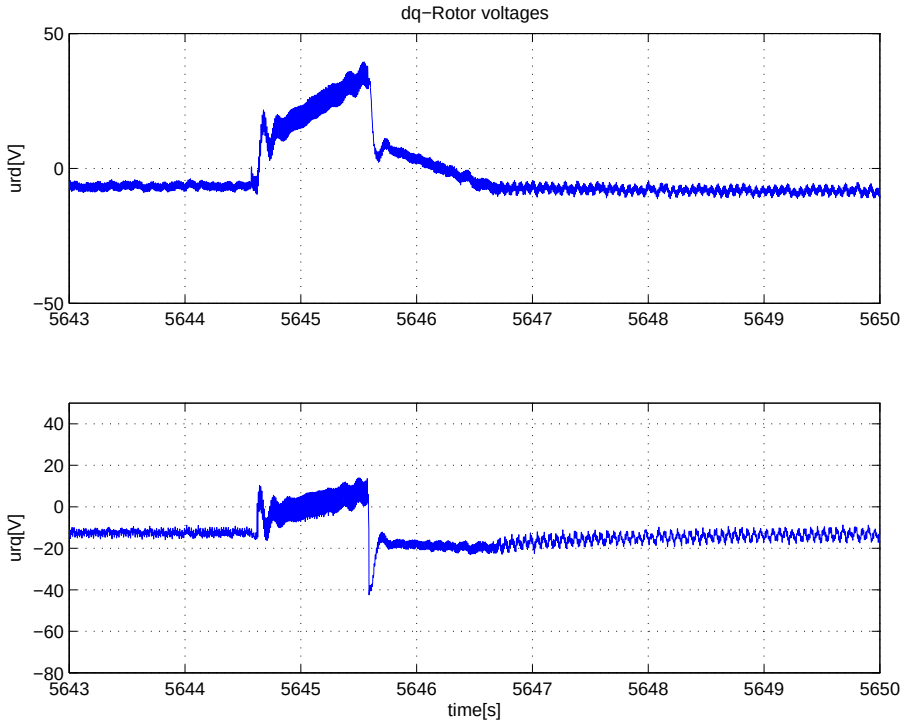

Figure 7: Experimental results: rotor dq-voltages, u_{rd} and u_{rq}.

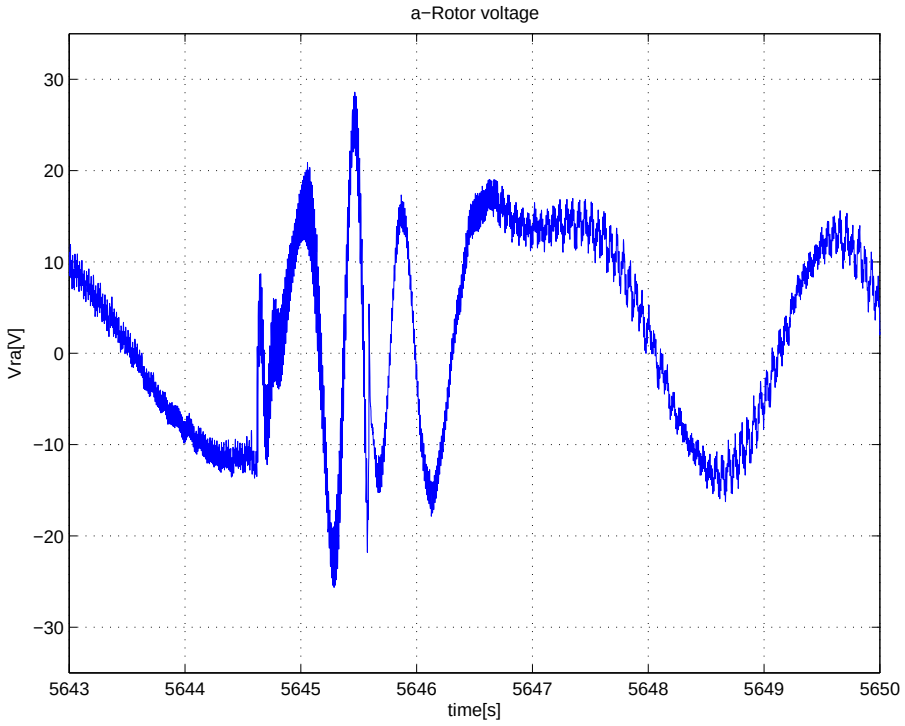

Figure 8: Experimental results: rotor a-voltage, V_{ra}.

goals of the system: to provide extra active power to a local load and to compensate the reactive power of the whole system.

The experiments contribute as well to validate the Port-Hamiltonian formalism and Bond Graph approach as an effective and usable tool to modelate complex/hybrid systems and the Hamiltonian passivity-based technique (IDA-PBC) as an algorithm to obtain controllers able to satisfy non standard requirements for non-linear systems.

References

[1] H. Akagi and H. Sato. Control and performance of a doubly-fed induction machine intended for a flywheel energy storage system. *IEEE Trans. Power Electron.*, 17(1):109–116, 2002.

[2] C. Batlle, A. Dòria-Cerezo, and R. Ortega. Power Flow Control of a Doubly–Fed Induction Machine Coupled to a Flywheel. *European Journal of Control*, 11(3):209–221, 2005.

[3] C. Batlle, A. Dòria-Cerezo, and E. Fossas. Geoplex d.4.3.3: Experimental setup: Generator and converter. Technical report, Universitat Politècnica de Catalunya - GeoPlex, 2006.

[4] A. Dòria-Cerezo. *Modeling, simulation and control of a doubly-fed induction machine controlled by a back-to-back converter*. PhD thesis, Universitat Politècnica de Catalunya, 2006.

[5] E. Hilton. *Manual for the Real Time Controls Laboratory, RTiC-Lab*, 2000.

[6] B. Hopfensperger, D. Atkinson, and R. Lakin. Stator-flux-oriented control of a doubly-fed induction machine with and without position encoder. In *IEE Proc. Electric Power Applications*, volume 147-4, pages 241–250, 2000.

[7] R. Peña, J. C. Clare, and G. M. Asher. Doubly fed induction generator using back-to-back pwm converters and its application to variable speed wind-energy generation. In *IEEE Proc. Electric Power Applications*, volume 143-5, pages 231–241, 1996.

[8] R. Peña, J. C. Clare, and G. M. Asher. A doubly fed induction generator using back-to-back pwm converters supplying an isolated load from a variable speed wind turbine. In *IEEE Proc. Electric Power Applications*, volume 143-5, pages 380–387, 1996.

[9] S. Peresada, A. Tilli, and A. Tonelli. Indirect Stator Flux-Oriented Output Feedback Control of a Doubly Fed Induction Machine. *IEEE Trans. Control Systems Technology*, 11(6):875–888, 2003.

[10] S. Peresada, A. Tilli, and A. Tonelli. Power control of a doubly fed induction machine via output feedback. *Control Engineering Practice*, 12:41–57, 2004.

[11] A. Tapia, G. Tapia, J. X. Ostolaza, and J. R. Sáenz. Modeling and control of a wind turbine driven doubly fed induction generator. *IEEE Trans. Energy Conversion*, 18:194–204, 2003.

[12] L. Xu and W. Cheng. Torque and reactive power control of a doubly fed induction machine by position sensorless scheme. *IEEE Trans. Industry Applications*, 31(3):636–642, 1995.